

18. Li, C., Brisco, B. B., Wang, R. J. and McDonald, J., SAR/TM wetland identification in the Lake St. Clair Delta. In Proc. 17th Canadian Symp. Remote Sensing, Canadian Remote Sensing Society, Ottawa, 1995, pp. 60–64.
19. Vibulsresth, S., Ratanasermpong, S., Dowreang, D. and Silapathong, C., Mangrove monitoring using satellite data. *TRSC Newslett.*, 1993, **10**, 1–2.
20. Venkataratnam, L., Thammappa, S. S. and Ravishankar, T., Mapping and monitoring prawn farming areas through remote sensing techniques. *Geocarto Int.*, 1997, **12**, 23–29.
21. Houhoulis, P. F. and Michener, W. K., Detecting wetland change: A rule-based approach using NWI and SPOT-XS data. *Photogramm. Eng. Remote Sensing*, 2000, **66**, 205–212.
22. Tripathi, N. K., Annachhatre, A. and Patil, A. A., On the role of remote sensing in environmental impact analysis of shrimp farming. Map India 2000, <http://www.gisdevelopment.net/application/miscellaneous/mis022pf.htm>
23. Markham, B. L. and Barker, J. L., Landsat MSS and TM post-calibration dynamic ranges, exoatmospheric reflectances and at-satellite temperatures. EOSAT Landsat Tech. Notes, vol. 1, pp. 3–8.
24. Bishop, Y., Fienberg, S. and Holland, P., *Discrete Multivariate analysis – Theory and Practices*, MIT Press, Cambridge, Massachusetts, 1975, p. 575.

ACKNOWLEDGEMENTS. We thank Dr R. R. Naval Gund, Director, and Dr P. S. Roy, Deputy Director, Remote Sensing and GIS Applications Area, National Remote Sensing Agency (NRSA), Hyderabad for providing financial support, necessary facilities and encouragement during the course of investigation. Thanks are also due to Marine Product Export Development Authority, Vijayawada for providing ancillary information. We are also grateful to Dr K. V. Ramana and S. Senthil Kumar, and G. Sujatha, NRSA for their technical support. Valuable comments and suggestions offered by the reviewer helped in improving the technical content of the article.

Received 10 February 2005; revised accepted 4 July 2005

Variations in terrigenous sediment discharge in a sediment core from southeastern Arabian Sea during the last 140 ka

J. N. Pattan^{1,*}, Toshiyuki Masuzawa² and Mineko Yamamoto³

¹National Institute of Oceanography, Dona Paula, Goa 403 004, India

²Department of Hydrospheric–Atmospheric Science, Graduate School of Environmental Studies and

³Hydrospheric–Atmospheric Research Centre, Nagoya University, Chikus-ku, Nagoya 464-8601, Japan

The bulk concentration (wt%) and mass accumulation rates (MAR; g/cm²/ka) of terrigenous source representing elements such as Al, Ti, K and Zr in a sediment core (SK-129/CR-05) from southeastern Arabian Sea, record considerable variations in riverine sediment discharge over the last 140 ka. The mean Al concentration ($4.51 \pm 0.47\%$) and its MAR ($0.105 \text{ g/cm}^2/\text{ka}$)

are higher during the glacial period and lower ($3.61 \pm 0.58\%$; $0.084 \text{ g/cm}^2/\text{ka}$) in the interglacial period. This suggests an increased terrigenous sediment discharge (TSD) of $\sim 25\%$ corresponding with chemical weathering (K/Al ratio) during glacials than in the interglacials. The last $\sim 5 \text{ ka}$ received lowest and uniform TSD (mean Al concentration $-2.36 \pm 0.06\%$; Al MAR, $0.075 \text{ g/cm}^2/\text{ka}$; K/Al ratio, 0.23 ± 0.003) may be due to weak monsoon and stabilized sea level. Marine Isotope Stage (MIS) – 1 and 4 recorded the lowest and highest TSD respectively. Interestingly, during MIS–5, interstadials (5.1, 5.3 and 5.5) were associated with relatively larger TDS, suggesting humid conditions and intense precipitation. On the contrary, stadials (5.2 and 5.4) were characterized by relatively smaller TDS, indicative of low precipitation and arid condition in the Indian subcontinent.

Keywords: Arabian Sea, marine environment, marine isotope stage, mass accumulation rate, terrigenous sediment discharge.

TERRIGENOUS sedimentation in the marine environment is mainly through fluvial or eolian pathways, which provides information about conditions on the continent and mechanisms of transport from continent to marine environment. The type and amount of terrigenous material depend on climatic conditions on the continent. About 95% of terrigenous material in the ocean reaches by the rivers and is deposited on continental margins¹. The elements and their transport pathways in the Arabian Sea suggest a number of sources, viz. detrital input from Somalia, aeolian from Arabia, detrital riverine input from Indus, Tapti and Narmada rivers and weathering of Deccan trap, gneissic rocks, laterites and submarine weathering of Carlsberg Ridge^{2–7}. The lithogenic input in the western Arabian Sea is largely eolian and is fluvial in the southeastern Arabian Sea^{4,8}, with a meagre aeolian fraction^{9,10}. Existing palaeoceanographic studies in the southeastern Arabian Sea are confined to productivity variation, clay mineralogy and hydrography changes^{11–18}, and variations of terrigenous input through geochemistry is not well recorded. In the present study, bulk concentration of terrigenous source elements (Al, Ti, K and Zr) and their mass accumulation rates (MAR; g/cm²/ka) are investigated in order to understand the variations of riverine sediment discharge in the southeastern Arabian Sea during the last 140 ka.

During the 129th cruise of *ORV Sagar Kanya* (Figure 1), a 5.52 m long gravity sediment core (SK-129/CR-05) was raised from southeastern Arabian Sea ($9^{\circ}21'N$: $71^{\circ}59'E$; water depth 2300 m). The sediment core was sub-sampled at 2 cm interval, dried and powdered in an agate mortar. *Globogerinoides ruber*, a planktonic foraminifera with a size range of 250–350 μm was used for oxygen isotope study and determination of calcium carbonate procedure has been published earlier¹⁹. For the chemical analyses of major and trace elements, the sediment was treated with a

*For correspondence. (e-mail: pattan@darya.nio.org)

mixture of HNO_3 , HClO_4 and HF in a PTFE vial using a microwave. After digestion, the solutions were evaporated to near dryness under infrared lamp on a hot plate in a draft chamber. The residue was brought into a clear solution with 2 M HNO_3 and final volume was made. These samples were analysed for Al, Ti, Fe, Na, K, Mg, Ba, Sr, Co, Cr, Li, Ni, Sc, V, Y, Zn and Zr with a Thermo Jarrel Ash IRIS-AP on a inductively coupled plasma-atomic emission spectrometry (ICP-AES). An international reference standard material (JB-2) supplied by Geological Survey of Japan²⁰ was used to check the accuracy, which was better than ± 5 for the elements analysed. Dry bulk density was calculated using the equation of Curry and Lohmann²¹. MAR were estimated by the individual element concentration, linear sedimentation rate (LSR) and dry bulk density. Element excess has been calculated following the equation: $[\text{Ele}_{\text{excess}} = \text{Ele}_{\text{total}} - (\text{Ti}_{\text{sample}} \times \text{Ele}/\text{Al}_{\text{shale}})]^{19}$.

The age model for the present sediment core is based on the oxygen isotope record of *G. ruber*¹⁹. This core covers a time span of 140 ka from late isotope stage 6 to the Present. The age model was derived by identifying globally recognizable isotopic events in the $\delta^{18}\text{O}$ records following Prell *et al.*²² and by assigning ages according to Martinson *et al.*²³. Linear interpolation between the oxygen isotope stage boundaries reveals variations in sedimentation rates between 3.67 and 5.20 cm/ka (average of 4.14 cm/ka)¹⁹, with highest sedimentation (5.2 cm/ka) during Marine

Isotope Stage (MIS)-4 and lowest (3.6 cm/ka) during MIS-3. During MIS-5, sedimentation rates varied from 0.8 to 7 cm/ka. Occurrence of high abundance of glass shards at 308 cm depth interval corresponds to Youngest Toba Tuff (YTT) of ~ 74 ka from northern Sumatra²⁴, matches well with the $\delta^{18}\text{O}$ chronology and confirms the interpolation of timescale derived from $\delta^{18}\text{O}$ stage boundaries are reasonable.

The calcium carbonate content in the core varies between 30 and 66%, with highest values (50 to 66%) during Holocene and a short pulse of high carbonate content (66%) during the early MIS-5 (Figure 2). The carbonate content during the last 5 ka is uniformly high (65%). Carbonate content during MIS-1, -3 and -5 is higher and during MIS-2, -4 and -6 is lower; this suggests increased productivity during interglacials than in the glacials. Similarly, other productivity proxies such as biogenic opal and biogenic Ba showed increased productivity during major interglacials¹⁹.

Aluminum shows a perfect positive correlation with Ti ($r = 0.99$, $n = 140$), suggesting sole supply from terrigenous source. Similarly, Al also shows a strong positive correlation with Li ($r = 0.97$), Zr ($r = 0.96$), K ($r = 0.93$), Sc ($r = 0.93$), Na ($r = 0.90$), Cr ($r = 0.89$), Mg ($r = 0.85$), V ($r = 0.85$) and Fe ($r = 0.70$), indicating their supply from a common source. The positive but comparatively poor correlation coefficient between Al and Fe ($r = 0.70$) compared to other terrigenous source elements could be due to the presence of excess Fe ($\sim 25\%$) (structurally unsupported) throughout the core. This excess Fe might have been supplied from the weathering of laterites from the hinterland, which in turn have been utilized in the formation of authigenic phases, such as verdine and glucony facies in the shelf²⁵ and pyrite, as observed in the present sediment core²⁴. Calcium carbonate, Sr and Ba exhibit positive correlation among themselves, suggesting a biogenic source and act as a dilutant to the detrital elements.

Clay mineralogy, seafloor sediment distribution and sediment trap data suggest that lithogenic fraction in the eastern Arabian Sea is largely fluvial in origin^{26,27}. MAR of Al, K, Ti and Zr ($\text{g}/\text{cm}^2/\text{ka}$) are indicative of terri-

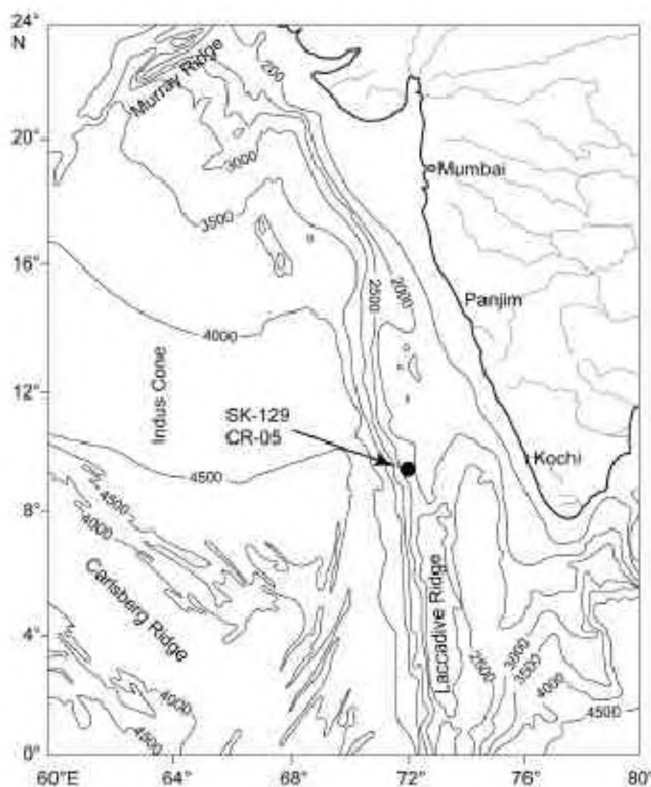


Figure 1. Location map showing position of a sediment core (SK-129/CR-05). Contours in metres.

Table 1. Mean Al (%) concentration, Al mass accumulation rate ($\text{g}/\text{cm}^2/\text{ka}$) and K/Al ratio during different marine isotope stages (MIS) in a sediment core (SK-129/CR-05) from southeastern Arabian Sea

Period (ka)	Al (%)	Al MAR ($\text{g}/\text{cm}^2/\text{ka}$)	K/Al ratio
Last 5 ka	2.36 ± 0.06 (06)	0.075	0.23 ± 0.003
0–12 (MIS-1)	2.78 ± 0.54 (14)	0.085	0.24 ± 0.015
12–24 (MIS-2)	4.37 ± 0.21 (12)	0.096	0.27 ± 0.004
24–59 (MIS-3)	4.03 ± 0.33 (32)	0.087	0.27 ± 0.012
59–75 (MIS-4)	4.80 ± 0.48 (21)	0.136	0.30 ± 0.025
75–129 (MIS-5)	3.53 ± 0.45 (49)	0.099	0.28 ± 0.021
129–141 (MIS-6)	4.32 ± 0.43 (12)	0.123	0.27 ± 0.009
Mean glacial	4.51 ± 0.47 (45)	0.105	0.28 ± 0.030
Mean interglacial	3.61 ± 0.58 (95)	0.084	0.26 ± 0.021

Total number of sediment samples analysed during each isotope stage is given in brackets.

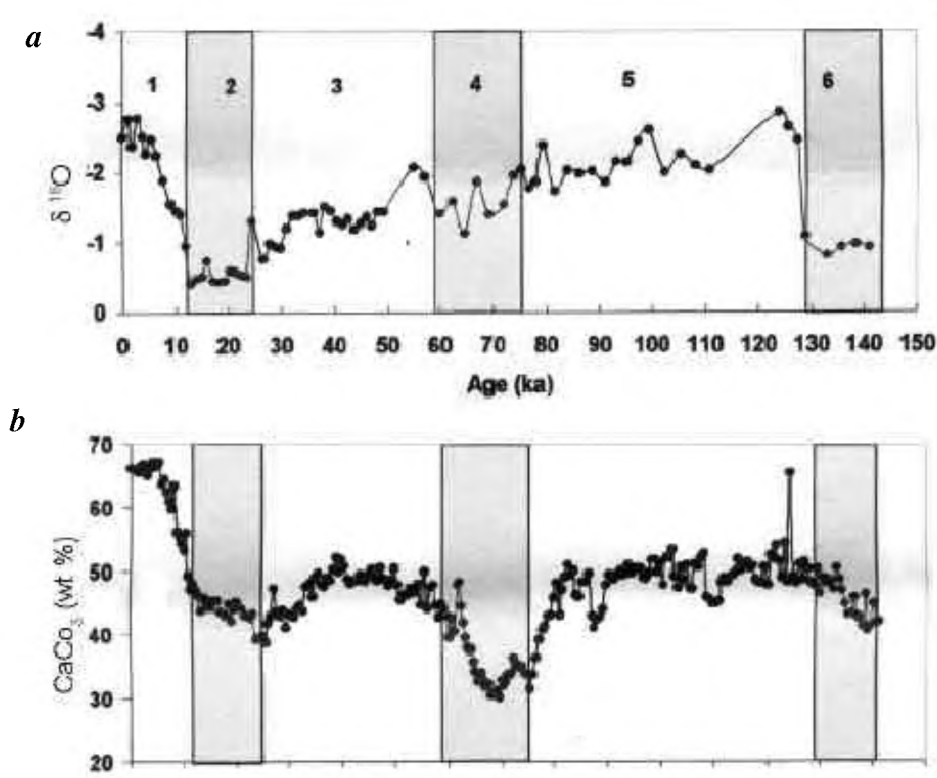


Figure 2. *a*, Oxygen isotope composition of *Globogerinoides ruber* in a sediment core (SK-129/GC-05) vs age (ka). Numbers 1–6 indicate marine isotope stages and shaded blocks are glacials. *b*, Distribution of calcium carbonate content in a sediment core (after Pattan *et al.*¹⁹).

genous sediment discharge (TSD) and their variations correspond well with each other for the last 140 ka (Figure 3). This implies that these elements may have been derived mainly from the same rock type. Table 1 shows the mean Al concentration, its MAR ($\text{g}/\text{cm}^2/\text{ka}$) and K/Al ratio during different isotope stages. The bulk Al concentration is high (average $4.51 \pm 0.47\%$) during glacial compared to interglacials (average $3.61 \pm 0.58\%$). Similarly, its MAR is also higher during glacials (average $0.105 \text{ g}/\text{cm}^2/\text{ka}$) than in the interglacials (average $0.084 \text{ g}/\text{cm}^2/\text{ka}$; Figure 3). This suggests $\sim 25\%$ increased TSD during glacials compared to interglacials in the southeastern Arabian Sea. Major rivers such as Indus, Tapti and Narmada and numerous small perennial rivers drain into the Arabian Sea, which brings continentally derived terrigenous material into the west coast of India. Higher terrigenous input during glacials could be due to low sea level and erosion of exposed shelf and draining of suspended river load directly into the deep sea. Sediment discharge decreases gradually from ~ 10 to ~ 5 ka. During the last 5 ka, sediment discharge was uniformly low (Figure 3 *a–c*), suggesting a weak monsoon and stabilized sea level²⁸. Similarly, reduced monsoon intensity during the last ~ 6 ka was inferred based on clay mineral supply¹⁵ and agrees with the previous studies^{29–32}. MIS boundary between 6 and 5 (termination-II) is marked by a distinct strong pulse of sediment discharge (Figure 3). Among the glacials, MIS-4 received highest

TSD compared to MIS-2 and MIS-1 which received the lowest TSD in the interglacials (Table 1, Figure 3). The high MAR of Al and K at ~ 75 ka could be due to the presence of YTT (Figure 3).

The high terrigenous flux suggests intensive hydrolysis resulting in enhanced erosion due to increased precipitation. In MIS-5, interstadials (5.1, 5.3 and 5.5) received reduced sediment discharge compared to stadials (5.2 and 5.4). A similar observation in the Niger Fan of Atlantic Ocean was attributed to the precessional variations, particularly 19 to 23 ka frequency band³³. The higher sediment discharge during interstadials suggests intense precipitation and humid condition. On the other hand, low sediment discharge during stadials is indicative of low precipitation and arid condition in the subcontinent. The low MAR (Figure 3 *c*) between 110 and 120 ka (MIS-5d) could have resulted due to low sediment accumulation rate¹⁹ and lack of oxygen isotope data points (Figure 2 *b*). MAR generally follow the LSR and this low MAR is not accompanied by corresponding elemental concentration (Figure 2 *a, b*). Therefore, we suspect that the low MAR during MIS-5d could be an artifact and may not be related to climatic changes.

Elemental fluxes depend upon the weathering intensity, which in turn is controlled by the vegetation coverage on the continents. Aluminum in the marine sediments is associated with fine-grained aluminosilicates or clays³⁴ and K is

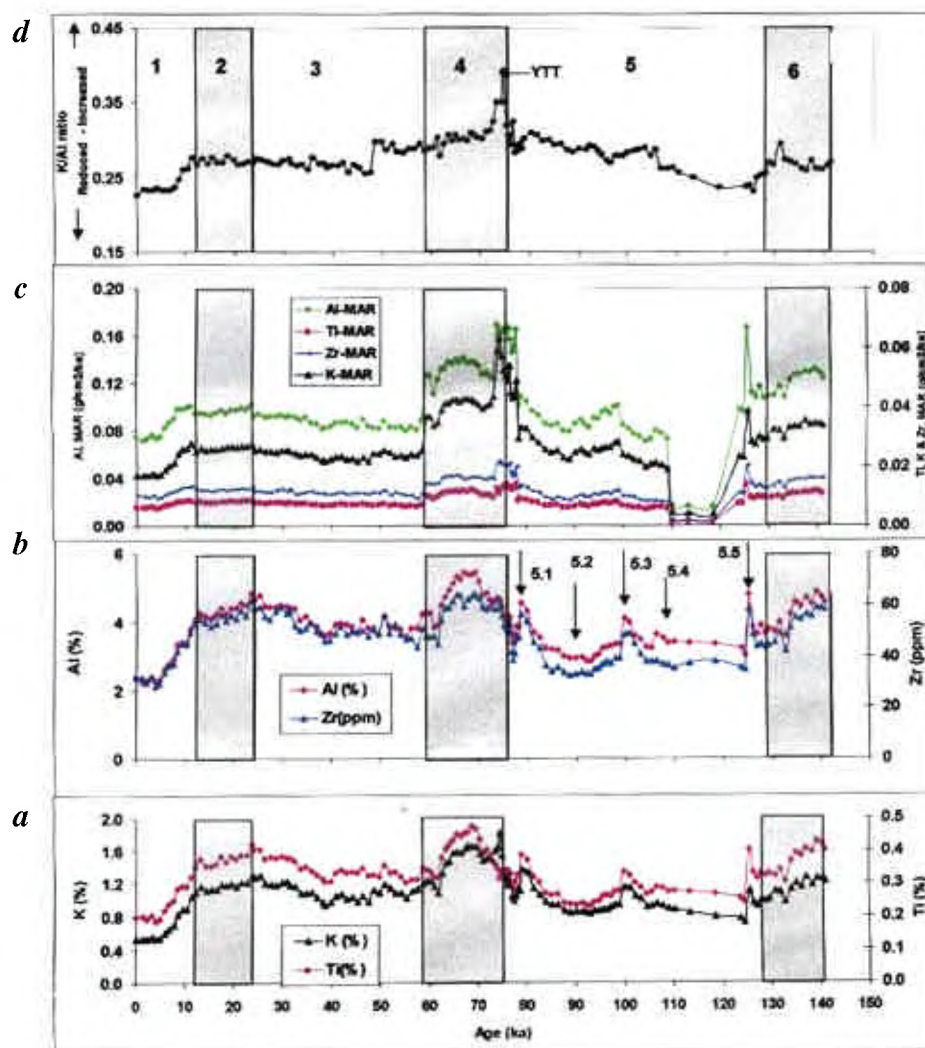


Figure 3a–c. Distribution of bulk concentration (%) and mass accumulation rates ($\text{g}/\text{cm}^2/\text{ka}$) of Al, Ti, K and Zr. **d.** K/Al ratio as an indicator of chemical weathering intensity in a sediment core (SK-129/GC-05) from south-eastern Arabian Sea during the last 140 ka. Numbers 1–6 indicate marine isotope stages. Shaded blocks are glacial periods. Arrows indicate interstadials and stadials. YTT; Youngest Toba Tuff.

associated with potash feldspar³⁵. The K/Al ratio, which represents illite³⁶, is used as a proxy for chemical weathering³⁴. The K/Al ratio in the present sediment core varies from 0.22 to 0.39 (Figure 3) and suggests high chemical weathering intensity (0.28) during glacial than during interglacials (0.26). The last 5 ka has recorded low and constant K/Al ratio ($0.23 \pm 0.003\%$), suggesting low chemical weathering due to weak monsoon. The highest K/Al ratio (0.39) at ~74 ka could be due to presence of YTT, where glass shards from the ash layer have high Al and low K content compared to the associated sediments²⁴.

1. Rea, D. K. and Leinen, M., Asian aridity and the zonal westerlies: Late Pleistocene and Holocene record of eolian deposition in the northwest Pacific Ocean. *Palaeogeogr. Palaeoclimatol. Palaeoecol.*, 1988, **66**, 1–8.

2. Nair, R. R., Hashmi, N. H. and Rao, V. P., Distribution and dispersal of clay minerals on the western continental shelf of India. *Mar. Geol.*, 1982, **50**, M1–M9.
3. Shankar, R., Subbarao, K. V. and Kolla, V., Geochemistry of surface sediments from the Arabian Sea. *Mar. Geol.*, 1987, **76**, 253–279.
4. Shimmield, G. B., Mowbray, S. R. and Weedon, G. P., A 350 ka history of the Indian southwest monsoon – evidence from deep sea cores, northwest Arabian sea. *Trans. R. Soc. Edinburgh: Earth Sci.*, 1990, **81**, 289–299.
5. Pederson, T., Shimmield, G. B. and Price, N. B., Lack of enhanced preservation of organic matter in sediments under the oxygen minimum on the Oman Margin. *Geochim. Cosmochim. Acta*, 1992, **56**, 545–551.
6. Sirocko, F. and Lange, H., Clay accumulation rates in the Arabian Sea during the late Quaternary. *Mar. Geol.*, 1991, **97**, 105–119.
7. Sirocko, F., Garbe-Schonber, D. and Devey, C., Processes controlling trace element geochemistry of Arabian Sea sediments during the last 25,000 years. *Glob. Planet. Change*, 2000, **26**, 217–303.

8. Paropkari, A. L., Geochemistry of sediments from the Mangalore–Cochin shelf and upper slope off southwest India: Geological and environmental factors controlling dispersal of elements. *Chem. Geol.*, 1990, **81**, 99–119.
9. Naidu, A. S., Mowatt, T. C., Somayajulu, B. L. K. and Rao, K. S. Characteristics of the clay minerals in the bed loads of major rivers of India. *Mitt. Geol.-Palaeontol. Inst. Univ., Hamburg*, 1985, **58**, 559–568.
10. Rao, V. P. and Rao, B. R., Provenance and distribution of clay minerals in the sediments of the western continental shelf and slope of India. *Cont. Shelf Res.*, 1995, **15**, 1757–1771.
11. Naidu, P. D., Glacial to interglacial contrasts in the calcium carbonate content and influence of Indus discharge in two eastern Arabian sea cores. *Palaeogeogr. Palaeoclimatol. Palaeoecol.*, 1991, **86**, 255–263.
12. Paropkari, A. L., Iyer, S. D., Chauhan, O. S. and Prakash Babu, C., Depositional environments inferred from variations of calcium carbonate, organic carbon and sulfide sulphur: A core from the southeastern Arabian Sea. *Geo-Mar. Lett.*, 1991, **11**, 96–102.
13. Thamban, M., Rao, V. P. and Raju, S. V., Controls on organic carbon distribution in the sediment cores from the eastern Arabian Sea. *Geo-Mar. Lett.*, 1997, **17**, 220–227.
14. Thamban, M., Rao, V. P., Schendier, R. R. and Groot, P. M., Glacial to Holocene fluctuations in hydrography and productivity along the southwestern continental margin of India. *Palaeogeogr., Paleoclimatol., Paleoecol.*, 2000, **165**, 113–127.
15. Thamban, M., Rao, V. P., Schendier, R. R. and Groot, P. M., Reconstruction of late Quaternary monsoon oscillations based on clay mineral proxies using sediment cores from the Western margin of India. *Mar. Geol.*, 2002, **186**, 527–539.
16. Sarkar, A., Bhattacharya, S. K. and Sarin, M. M., Geochemical evidence for anoxic deep water in the Arabian sea during the last glaciation. *Geochim. Cosmochim. Acta*, 1993, **57**, 1009–1016.
17. Sarkar, A., Ramesh, R., Bhattacharya, S. K. and Price, N. B., Paleomonsoon and paleoproductivity records of $\delta^{18}\text{O}$, $\delta^{13}\text{C}$ and CaCO_3 variations in the northern Indian Ocean sediments. *Proc. Indian Acad. Sci. (Earth Planet. Sci.)*, 2000, **109**, 157–169.
18. Bhusan, R., Dutta, K. and Somayajulu, B. L. K., Concentrations and burial fluxes of organic and inorganic carbon on the eastern margins of the Arabian Sea. *Mar. Geol.*, 2001, **178**, 95–113.
19. Pattan, J. N., Masuzawa, T., Divakar Naidu, P., Parthiban, G. and Yamamoto, M., Productivity fluctuations in the southeastern Arabian Sea during the last 140 ka. *Paleogeogr. Paleoclimatol. Paleoecol.*, 2003, **193**, 575–590.
20. Imai, N., Terashima, S., Itoh, S. and Ando, A., 1994 compilation values for GSJ reference samples, 'Igneous rock series'. *Geochim. J.*, 1995, **29**, 91–95.
21. Curry, W. B. and Lohmann, G. P., Late Quaternary carbonate sedimentation at the Sierra Leone Rise (eastern equatorial Atlantic Ocean). *Mar. Geol.*, 1986, **70**, 223–250.
22. Prell, W. L., Imbrie, J., Martinson, D. G., Morley, J. J., Pisias, N. G., Shackleton, N. J. and Streeter, H. F., Graphic correlation of oxygen isotope stratigraphy application to the late Quaternary. *Paleoceanography*, 1986, **1**, 137–162.
23. Martinson, D. G., Pisias, N. G., Hays, J. D., Imbrie, J., Moore, T. C. and Shackleton, N. J., Age dating and the orbital theory of the ice ages: Development of a high resolution 0 to 300,000 year. *Quat. Res.*, 1987, **27**, 1–29.
24. Pattan, J. N., Shane, P., Pearce, N. J. G., Banakar, V. K. and Parthiban, G., An occurrence of ~ 74 ka Youngest Toba Tephra from the Western Continental Margin of India. *Curr. Sci.*, 2001, **80**, 1322–1326.
25. Rao, V. P., Lamboy, M. and Dupeable, P. A., Verdine and other associated authigenic (glaucony, phosphate) facies from the surficial sediments of the southwestern continental margin of India. *Mar. Geol.*, 1993, **111**, 133–158.
26. Kolla, V., Kostecki, J. A., Robinson, F., Biscaye, P. E. and Ray, P. K., Distributions and origins of clay minerals and quartz in surface sediments of Arabian Sea. *J. Sediment. Petrol.*, 1981, **51**, 563–569.
27. Nair, R. R. *et al.*, Increased particle fluxes to the oceans related to the monsoons. *Nature*, 1989, **338**, 749–751.
28. Fairbanks, R. G., A 17,000 year glacio-eustatic sea level record: influence of glacial melting rates on the Younger Dryas event and deep-ocean circulation. *Nature*, 1989, **342**, 637–642.
29. Bayson, R. A. and Swain, A. M., Holocene variations of monsoon rainfall in Rajasthan. *Quat. Res.*, 1981, **16**, 135–145.
30. Van Campo, E., Monsoon fluctuations in two 20,000 yr BP oxygen-isotope/pollen records off southwest India. *Quat. Res.*, 1986, **26**, 376–388.
31. Rajagopal, G., Sukumar, R., Ramesh, R. and Pant, R. K., Late Quaternary vegetational and climatic changes from tropical peats in southern India – An extended record up to 40,000 years BP. *Curr. Sci.*, 1997, **73**, 60–63.
32. Enzel, Y. *et al.*, High resolution Holocene environmental changes in the Thar Desert, Northwestern India. *Science*, 1999, **284**, 125–128.
33. Zabel, M., Scheider, R. R., Wagner, T., Adegbe, T., Vries, Uwe de and Kolonic, S., Late Quaternary climate changes in Central Africa as inferred from terrigenous input to the Niger fan. *Quat. Res.*, 2001, **56**, 207–217.
34. Calvert, S. E., The mineralogy and geochemistry of near-shore sediments. In *Treatise on Chemical Oceanography* 6 (eds Riley, J. P. and Chester R.), Academic Press, San Diego, 1976, pp. 187–280.
35. Shimmield, G. B. and Mowbray, S. R., The inorganic geochemical record of the northwest Arabian sea: A history of productivity variation over the last 400 ka from sites 722 and 724. In *Proceedings of Ocean Drilling Program Science Results*, 1991, vol. 117, pp. 409–429.
36. Yarinick, K. M., Murray, R. W. and Peterson, L. C., Climatically sensitive eolian and hemipelagic deposition in the Cariaco Basin, Venezuela over the past 578,000 years. *Palaeoceanography*, 2000, **15**, 210–218.

ACKNOWLEDGEMENT. J.N.P. thanks Japan Society for the Promotion of Science for fellowship. This is NIO contribution no. 4042.

Received 23 December 2004; revised accepted 16 June 2005